



ELSEVIER

Available online at www.sciencedirect.com

SCIENCE @ DIRECT®

Nuclear Instruments and Methods in Physics Research A 539 (2005) 445–454

NUCLEAR
INSTRUMENTS
& METHODS
IN PHYSICS
RESEARCH
Section A

www.elsevier.com/locate/nima

Mode analysis of a multilayered dielectric-loaded accelerating structure

Chunguang Jing^{a,*}, W.M. Liu^a, W. Gai^a, J.G. Power^a, Thomas Wong^b

^aHigh Energy Physics Division, Argonne National Laboratory, F249, Bldg. 362, 9700S Cass AVE, Argonne, IL 60439, USA

^bElectrical and Computer Engineering Department, Illinois Institute of Technology, Chicago, IL 60616, USA

Received 6 July 2004; received in revised form 15 October 2004; accepted 24 October 2004

Available online 21 December 2004

Abstract

In this paper we evaluate a cylindrical metallic waveguide lined with multiple layers of dielectric for use as a slow-wave microwave accelerating structure. A general analysis of this traveling wave, multilayered, dielectric-loaded accelerating structure is presented including field solutions for both the TM (acceleration) modes and HEM (parasitic) modes. Furthermore, we present a recursive design procedure for choosing the layer thicknesses, calculation of the standard accelerator figures of merit such as the quality factor Q and shunt impedance per unit length r , and an easy to implement method for damping the HEM modes. Most importantly, it is shown that this multilayered DLA structure has a dramatically improved attenuation compared to the conventional single-layered dielectric-loaded structure while maintaining comparable shunt impedance. As a numerical example, we compare an 11.424 GHz multilayered structure using 4 layers and an 11.424 GHz conventional single-layered structure.

© 2004 Elsevier B.V. All rights reserved.

PACS: 41.75.Lx; 41.20.Jb

Keywords: Multilayer; Dielectric-loaded accelerator; Bragg fiber

1. Introduction

The conventional dielectric-loaded accelerating (DLA) structure [1–3] consists of a dielectric-lined cylindrical waveguide of inner radius $r = b_0$, outer radius $r = b_1$, length L , and dielectric constant ϵ

driven by an external microwave source. This structure can be operated as a slow-wave, traveling wave (TW) accelerator by adjusting b_0 , b_1 , and ϵ until the phase velocity is c . While the conventional DLA scheme has great potential as an advanced accelerating device, a major concern for it is its relatively high field attenuation per unit length, α_0 . This is caused by strong magnetic fields at the metal wall ($r = b_1$) which in turn gives rise to large surface currents and hence large attenuation.

*Corresponding author. Tel.: +1 630 252 0586;
fax: +1 630 252 5076.

E-mail address: jingchg@hep.anl.gov (C. Jing).

Normally, one prefers high dielectric constant materials to keep the group velocity of the wave low ($v_g \approx 1/\epsilon$) since that maximizes shunt impedance per unit meter, however, high dielectric constant materials further increase the attenuation. Our challenge is then to find a way to reduce the attenuation while simultaneously keeping the shunt impedance high.

Previous work in the optical regime on the Bragg Fiber (a hollow-core, multilayered, dielectric-lined cylindrical waveguide) has shown that this device is capable of low-loss and high-power transmission. It has found applications in both low-loss communications [4–9] and the high-power laser transmission [10,11]. Theoretical efforts to apply the Bragg Fiber concept to communications can be traced back to Yeh and Yariv [4], and more recent works by Xu et al. [8,9]. Their work provides us with a general method for solving for the modes in a cylindrical waveguide consisting of radially periodic layers of dielectrics. The Bragg Fiber has also been applied to high-power transmitting waveguide for lasers as shown in Refs. [10,11], where the authors have used a transmission line model to calculate the wave attenuation value for certain guided modes. In all of the above analysis, however, the work was confined to non-accelerating TE or HEM modes.

The idea of using the Bragg Fiber as an optical accelerator (the Optical Bragg Accelerator) has been previously analyzed by Schächter et al. [12] and Mizrahi et al. [13]. Their motivation was to design an all-dielectric accelerator (i.e. one that uses no outer metal jacket) since dielectrics are known to sustain higher electric fields than metals in the optical regime. In the Optical Bragg Accelerator, the dielectric layers are used to create multiple reflections in order to confine the accelerating TM fields without using a metallic outer jacket. In another study, a five zone rectangular DLA structure was studied by Wang et al. [14] which used two vacuum layers to reduce the wall losses.

In this paper, we will extend the Bragg Fiber concept to the microwave regime in order to develop low-loss accelerating structures with high shunt impedance. We call this microwave device the multilayered DLA structure (Fig. 1). It has a

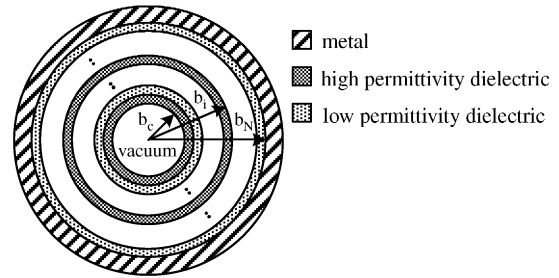


Fig. 1. Cross-section of the multilayered DLA structure. The structure is cylindrical waveguide which consists of vacuum core with radius b_0 surrounded by alternative high or low permittivity dielectric tubes with outer radius b_i , and outmost metal jacket.

vacuum channel of radius b_0 , surrounded by multiple dielectric layers in a cylindrical metallic waveguide of radius b_N . The dielectric layers serve as multiple reflectors that are used to reduce the magnetic field strength on the copper wall, thus making it possible to reduce the wall losses, and hence, the attenuation. However, instead of trying to achieve total field confinement of the leaky modes with an all dielectric structure (which requires many dielectric layers), here we use the multiple layers to reduce the attenuation to an acceptable level, while total confinement is achieved by the metallic wall. A modal analysis of the multilayered DLA structure is presented in Section 2 along with the general design procedure for obtaining low losses. In Section 3, the general parameters of the multilayer DLA structure for the accelerating TM modes and parasitic HEM modes (which when excited by off-axis particles cause transverse wakefields) are calculated and the particular parameters for a 4-layer DLA structure worked out to demonstrate the design procedure for choosing the accelerating mode. In Section 4, an effective and easy method for damping the HEM modes is discussed.

2. Mode analysis

Consider the multilayered DLA structure shown in Fig. 1. A hollow vacuum core of radius $r = b_0$ is surrounded by periodic dielectric layers with radius $b_i (i = 1, 2, \dots, N)$ and alternating permittivity (ϵ_{low}

and $\varepsilon_{\text{high}}$), and the outer most dielectric layer is covered by metallic jacket at $r = b_N$. Unlike power transmission applications, here only the properties of the synchronous modes (phase velocity equal to particle velocity, typically close to the speed of light, c) are of interest. For a given RF frequency of accelerator operation, the radius b_i of each layer is determined by the synchronous condition and dielectric constants ε_i . One can optimize the accelerator properties by varying the b_i and ε_i .

2.1. Recursive field relations

Modes supported by the multilayered DLA structure are either TM_{0n} , TE_{0n} , or HEM_{mm} modes (HE and EH). The general solutions for the longitudinal component of the electric and magnetic fields for the i th dielectric layer are:

$$\begin{aligned} E_{zi}(z, r, \phi) &= [A_i J_m(k_i r) + B_i Y_m(k_i r)] e^{jm\phi} e^{j(\omega t - \beta z)} \\ H_{zi}(z, r, \phi) &= [C_i J_m(k_i r) + D_i Y_m(k_i r)] e^{jm\phi} e^{j(\omega t - \beta z)} \end{aligned} \quad (1)$$

where

$$\begin{aligned} k_i &= \omega \sqrt{\frac{\mu_{ri} \varepsilon_{ri}}{c^2} - \frac{1}{v_p^2}} \\ \beta &= \omega^2 \mu_0 \varepsilon_0 \mu_{ri} \varepsilon_{ri} - k_i^2. \end{aligned} \quad (2)$$

v_p is the phase velocity of the wave, c is speed of light in vacuum, k_i is the transverse wave number in the i th layer, β is the propagation constant along the z -axis, and μ_{ri} and ε_{ri} are the relative permeability and permittivity for the i th layer, respectively. The transverse field components can be derived from the fields given by Eq. (1):

$$\begin{aligned} E_{ri} &= \frac{-j}{k_i^2} \left(\beta \frac{\partial E_{zi}}{\partial r} + \frac{\omega \mu_i}{r} \frac{\partial H_{zi}}{\partial \phi} \right) \\ E_{\phi i} &= \frac{-j}{k_i^2} \left(\beta \frac{\partial E_{zi}}{\partial \phi} - \omega \mu_i \frac{\partial H_{zi}}{\partial r} \right) \\ H_{ri} &= \frac{j}{k_i^2} \left(\frac{\omega \varepsilon_i}{r} \frac{\partial E_{zi}}{\partial \phi} - \beta \frac{\partial H_{zi}}{\partial r} \right) \\ H_{\phi i} &= \frac{-j}{k_i^2} \left(\omega \varepsilon_i \frac{\partial E_{zi}}{\partial r} + \frac{\beta}{r} \frac{\partial H_{zi}}{\partial \phi} \right). \end{aligned} \quad (3)$$

In each layer, there are four unknown coefficients A_i , B_i , C_i , and D_i . By applying the boundary

condition at each of the radial boundaries, a 4×4 transfer matrix M [15], which stands for the recurrence relation from the i th layer to the $(i + 1)$ th layer, is obtained as

$$\begin{pmatrix} A_{i+1} \\ B_{i+1} \\ C_{i+1} \\ D_{i+1} \end{pmatrix} = M \begin{pmatrix} A_i \\ B_i \\ C_i \\ D_i \end{pmatrix}, \quad i = 0, \dots, N-1. \quad (4)$$

At $r = 0$ we require that B_0 and D_0 to be zero. We then have $(4 \times N) + 2$ unknown constants and $4 \times N$ equations for the multilayer DLA structure. The additional two equations come from the boundary conditions at inner surface of metallic wall, $Ez(r = b_N) = Hr(r = b_N) = 0$. Now, by applying the recurrence relation (Eq. (4)), a simplified equation can be derived,

$$\begin{pmatrix} A_N \\ B_N \\ C_N \\ D_N \end{pmatrix} = M_{N-1} \cdots M_1 M_0 \begin{pmatrix} A_0 \\ 0 \\ C_0 \\ 0 \end{pmatrix} \quad (5a)$$

with

$$\begin{aligned} A_N J_m(k_N b_N) + B_N Y_m(k_N b_N) &= 0 \\ C_N J'_m(k_N b_N) + D_N Y'_m(k_N b_N) &= 0 \end{aligned} \quad (5b)$$

where M_i , ($i = 0, 1, \dots, N-1$) is the transfer matrix for the i th boundary, and b_N is radius to the inner surface of metal wall. If we know the electric and magnetic fields in any particular layer, then the unknown coefficients for any other dielectric layer can be calculated through this transfer matrix. The condition for a non-trivial solution to Eq. (5) will determine the dispersion relation of this waveguide. By normalizing either the initial electric or magnetic field and combining Eq. (2), the ω - β relation for the different modes can be found. As usual, the modes are represented by the orders of Bessel functions m and different number of roots n . For example, if the order of the Bessel functions m equals zero, then the transfer matrix M_i is reduced to a diagonal block, which represents two categories of degenerate modes— TM_{0n} and TE_{0n} , where the subscript n is the n th of root for Eq. (5). Otherwise, the hybrid modes HEM_{mm} , with all six field components, are obtained from $m > 0$.

While TE modes are of primary interest in optical transportation applications, we ignore these modes since they cannot accelerate charged particles. Instead, we will concentrate on the accelerating modes (TM_{0n}) and some of the parasitic modes (HEM_{1n}) since they can be excited by the charged particles.

2.2. Optimization procedure

Before computing the accelerator characteristics of the multilayer DLA structure, we need to find the optimal thickness of each dielectric layer. As stated at the beginning of this paper, the motivation for considering the multilayer DLA structure was to decrease the field attenuation by reducing the magnetic field at the metal wall. Borrowing the optimization procedure for the Bragg fiber [4,9], we can accomplish this by reducing the fields in the outward direction much faster than in the single-layer dielectric structure. In other words, we can optimize the structure to have much weaker fields at the wall. For the TM_{0n} mode, this optimization criteria is

$$\begin{cases} H_{\phi}(r = b_i) = E'_z(r = b_i) = 0 & \text{if } k_{i+1} < k_i \\ H'_{\phi}(r = b_i) = E_z(r = b_i) = 0 & \text{if } k_{i+1} > k_i \end{cases} \quad (6)$$

where the prime represents differentiation in the radial direction. Before optimization, implicit parameters in the transfer matrix M_i , such as frequency, phase velocity and the alternating dielectric constants, should be set. The minimum radius of the vacuum region b_0 is determined by the beam size and is not adjusted during this optimization. Then by replacing the outermost conductor boundary condition in Eq. (5) with Eq. (6) and implement Eq. (6) into the boundary condition of each layer, the radius of boundary b_i can be easily obtained by sequential outward solving of Eq. (5).

Plots of the longitudinal electric field for several TM (Fig. 2a) and HEM (Fig. 2b) modes supported in a 4-layer ($N = 4$) dielectric-loaded metallic waveguide. In this example, we set the permittivity for the dielectric layers as 20 and 10, $b_0 = 3$ mm and the found optimized dimensions as $b_1 = 5.99$ mm, $b_2 = 8.3$ mm, $b_3 = 9.8$ mm, and $b_4 = 12.1$ mm. The field amplitude of each mode is normalized to its field in the vacuum region when

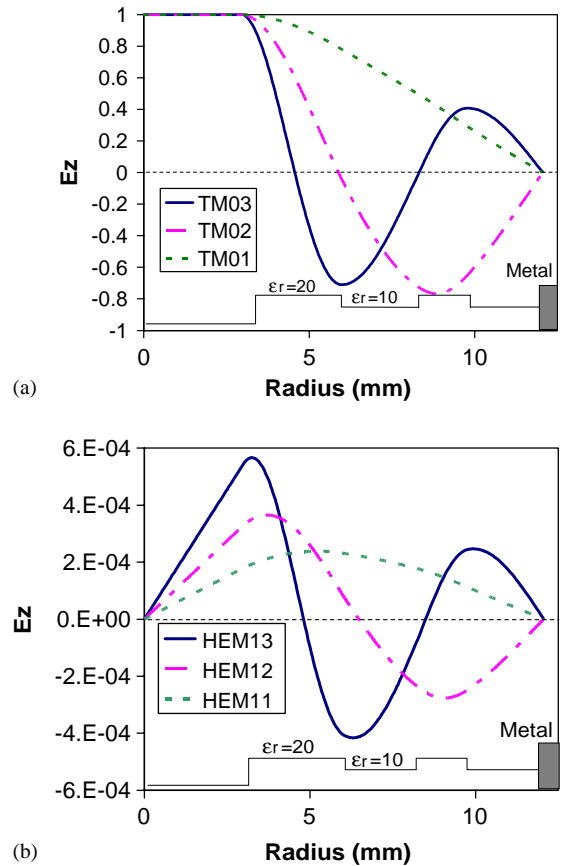


Fig. 2. Profile of longitudinal electric fields for several TM modes (a) and parasitic modes (b) built in a 4-layer dielectric-loaded accelerating structure in which TM_{03} mode is chosen as accelerating mode. Where, the permittivity for alternative dielectric layers is 20 and 10, and radius of each dielectric layer is $b_0 = 3$ mm, $b_1 = 5.99$ mm, $b_2 = 8.3$ mm, $b_3 = 9.8$ mm, and $b_4 = 12.1$ mm, respectively.

synchronized. For the multilayer DLA structure, the usual operating mode for particle acceleration is no longer the fundamental mode, TM_{01} . In this case, in order to minimize the power losses while maintaining other accelerating properties, the accelerating mode is chosen to be TM_{03} , which has its synchronized frequency at 11.424 GHz.

The dispersion curves of several modes for the same structure are shown in Fig. 3. The synchronous frequency for each mode can be obtained at the intersection point between each curve and the light line. And all important accelerating para-

meters are calculated using those synchronous frequencies. Fig. 4 provides another view to see how the field of the accelerating mode TM_{03} is intensely confined inside the vacuum region by bragg reflecting layers. That means that we can obtain higher Q or lower power loss than that for the other modes. Fig. 4 also shows that, like single-layer DLA structure, the multilayer DLA structure also has good field confinement for high order

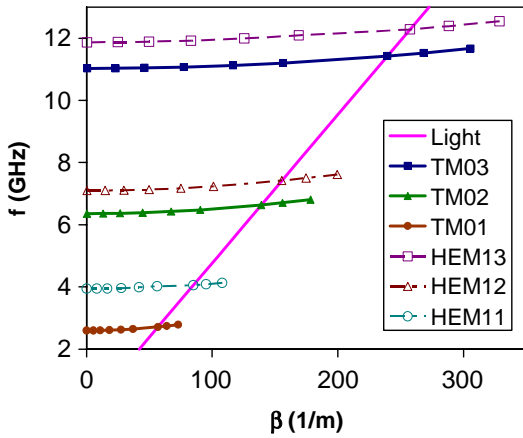


Fig. 3. Dispersion relations of several low order modes in 4-layer dielectric-loaded metallic cylindrical waveguide with same dimension as Fig. 2.

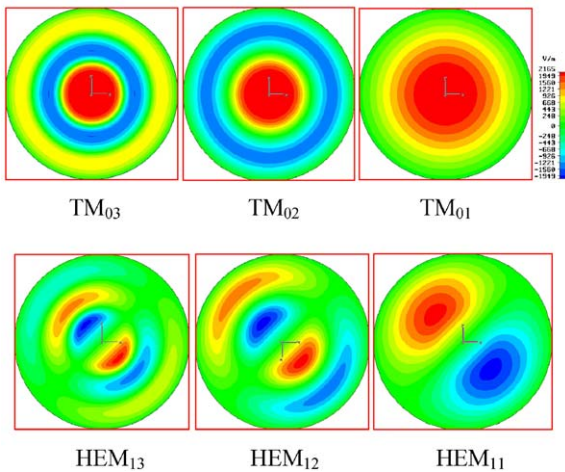


Fig. 4. Longitudinal electric field distribution of some lower order modes in cross-section of the 4-layer dielectric-loaded waveguide which has same dimensions as shown in Fig. 2.

hybrid mode HEM_{13} (parasitic mode), which may exert transverse force on off-center particles. However, we can use Chojnacki scheme [16] to damp those parasitic modes effectively. This will be discussed in Section 4.

3. Accelerator properties

To discuss or furthermore compare the different accelerating structures quantitatively, it is helpful to introduce some commonly used accelerator properties related parameters. In this section, we will calculate some standard accelerator figures of merit and compare the multilayered DLA structure to the single-layered DLA structure to show the advantages of the former.

We first begin by reminding the reader of some of the basic figures of merit for a TW structure. There parameters are: the group velocity v_g , the shunt impedance per unit length r , the attenuation constant per unit length α_0 , and the ratio of the shunt impedance per unit length to the quality factor (r/Q) and are defined [17] as

$$v_g = \frac{d\omega}{d\beta} = \frac{P}{U} \tag{6a}$$

$$\frac{r}{Q} = \frac{E_a^2}{\omega U} \tag{6b}$$

$$r = \frac{E_a^2}{-dP/dz} \tag{6c}$$

$$\alpha_0 = \frac{\omega}{2Qv_g} \tag{6d}$$

where P and U represent the TW power (energy flow) in the structure and the time-averaged stored energy per unit length in the structure, respectively,

$$P = \frac{1}{2} \oint_S \vec{E} \times \vec{H}^* \cdot d\vec{s} \tag{7a}$$

$$U = \frac{\epsilon}{4} \text{Re} \left(\int_V \vec{E} \times \vec{E}^* \cdot d\vec{v} \right) + \frac{\mu}{4} \text{Re} \left(\int_V \vec{H} \times \vec{H}^* \cdot d\vec{v} \right) \tag{7b}$$

and v_g is group velocity, Q is quality factor, and E_a is acceleration gradient. Based on the above definitions, we see that all of the acceleration parameters are connected to one another.

The shunt impedance per unit length, r , is a measure of the effectiveness of producing an axial accelerating field amplitude, E_a , for a given power dissipated per unit length $-dP_{\text{loss}}/dz$, (which is equal to $-dP/dz$). In particular, for a constant impedance TW accelerator, r is related to particle energy gain ΔW within an accelerating distance L and can be expressed as [17]

$$\Delta W = q\sqrt{rP_0L} \frac{1 - e^{-\alpha_0L}}{\sqrt{\alpha_0L}} \cos \varphi \quad (8)$$

where P_0 is incident RF power, and φ is the particle phase relative to the crest of the RF wave.

Another useful figure of merit is the so-called r over Q (r/Q) which measures the efficiency of acceleration, E_a , per unit stored energy, U , at a given frequency, ω . Combining Eqs. (6a) and (6b) we get

$$E_a^2 = P \frac{r}{Q} \frac{\omega}{v_g} \quad (9)$$

which shows that for a given incident power the accelerating gradient, E_a , is proportional to r/Q and inversely proportional to group velocity, v_g . This means that even when a structure has a high r/Q , it may not be an efficient accelerator if v_g is also high. Aside from using r/Q to characterize the accelerating efficiency of a constant impedance TW accelerator, once we know r/Q of each mode [18,19], it also reveals the amplitude of the wakefields generated by charged particles traveling through the structure without having to solve the inhomogeneous Maxwell's equations. In Eq. (6d), α_0 , is defined as field attenuation per unit length, which satisfies

$$P(z) = P_0 e^{-2\alpha_0 z} \quad (10)$$

where P is traveling wave power (energy flow) and z is the direction of propagation.

According to Eq. (9), for a given incident RF power, P_0 , a high accelerating gradient, E_a , is obtained when r/Q is big and v_g is small. However, according to Eq. (6d), we want v_g high to keep the RF power attenuation, α_0 , small and thus reduce

the drop in the accelerating gradient along the structure length. For a constant-impedance, TW structure, the maximally efficient particle acceleration may be evaluated with Eq. (8), in which shunt impedance dominates particle energy gain after the structure length is optimized [17].

3.1. Numerical example: A 4-layer multilayer DLA structure

In this section, we give an example of an X-band multilayer DLA structure with 4-layers ($N = 4$). The first column in Table 1 summarizes the characteristic parameters of this structure. Note that the Quality factor Q is computed based on only the copper wall losses since we assume that an extremely low loss dielectric material may be obtained. These same parameters were also calculated for a single-layer DLA structure in the second column of Table 1. Comparison between the 4-layer and the single-layer structures shows that both r and α_0 have been improved remarkably. Even though r/Q becomes smaller, due to much higher Q , than that of the single-layer DLA structure, the 4-layer structure still has comparable number referring to the all metal structure. More significantly, the shunt impedance has been improved from 25 to 89 M Ω /m, which means the particle is accelerated much more efficiently.

After reading the above, the reader may suspect that the improved performance of the multilayered structure is not due to its multiple layers, but rather the choice of the TM_{03} mode as the accelerating mode. To demonstrate that this is not the case, we also calculated the corresponding parameters of the TM_{03} mode for the single-layer structure as shown in the third column of Table 1. As usual, the outside radius of single-layer, b_1 , was chosen to make the TM_{03} mode synchronous at 11.424 GHz. Table 1 shows that r is similar to that of the TM_{01} mode, which means that there is no improvement in the accelerator efficiency, even though Q was noticeably increased. This is because, instead of reduction of the wall loss, the increase in Q was mostly the result of the increase in stored energy per unit length, U , due to the increased volume. But for multilayer DLA

Table 1
Accelerating modes RF parameters comparison for different DLA structures

	4-layer accelerating mode (TM ₀₃)	Single-layer accelerating mode (TM ₀₁)	Single-layer accelerating mode (TM ₀₃)
Cut-off freq. (GHz)	11.03	11.1	11.13
Synchronized freq. (GHz)	11.424	11.424	11.424
Group velocity ($\times c$)	0.068	0.055	0.051
Q	33476	2865	12551
r (M Ω /m)	89	25.1	25.1
r/Q (Ω /m)	2658	8756	2007
Power attn (dB/m)	0.45	6.6	1.6

Geometric parameters for 4-layer DLA structure: radius of each layer is, in sequence, $b_0 = 3$ mm, $b_1 = 5.99$ mm, $b_2 = 8.3$ mm, $b_3 = 9.8$ mm, $b_4 = 12.1$ mm; single-layer DLA structure using TM₀₁ as accelerating mode: $b_0 = 3$ mm, $b_1 = 4.567$ mm; single-layer DLA structure using TM₀₃ as accelerating mode: $b_0 = 3$ mm, $b_1 = 10.57$ mm (choose different outmost radius is to keep same synchronized frequency for different accelerating mode).

structure, due to the suppressed fields as a ratio of the transverse cut-off wave number k_i to k_{i+1} in the periodic bragg reflectors (Eq. (6)), the power dissipated in the copper wall was decreased and therefore the shunt impedance improved dramatically.

In Section 2 we described the procedure to determine the radius of each dielectric layer except for that of the radius of vacuum core, b_0 . While the lower limit of b_0 is set by the beam size, this does not mean that we can choose an arbitrary core size as long as it is above this lower limit. Fig. 5 shows how b_0 influences the four accelerating parameters described above. Basically, increasing b_0 makes r and r/Q worse, but without much of an effect on v_g and α_0 . A second factor which has a significant effect on all four parameters is the ratio of dielectric constants, $\epsilon_{\text{high}}/\epsilon_{\text{low}}$, in the alternating dielectric layers. For a given b_0 , a large ratio of $\epsilon_{\text{high}}/\epsilon_{\text{low}}$ improves r , r/Q and α_0 but increases v_g significantly. Fig. 5 shows these effects when b_0 is varied from 2.5 to 5 mm. Lastly, the value of the absolute value of the dielectric constant in both layers should be kept high since the thickness of dielectric layer is related to the guided wave length and a higher dielectric constant makes the radius of whole structure smaller. By inspection Fig. 5, we can choose the optimal accelerating features.

4. Parasitic mode damping

When an off-axis particle travels through the multilayer DLA structure, parasitic, HEM modes will be excited which can impart transverse deflection forces to trailing particles and degrade the beam quality if they are not sufficiently suppressed. In the case of an iris-loaded (metal) accelerating structure, manifolds can be used to damp the parasitic modes. For a DLA structure, we use the method presented in Ref. [16] to suppress the HEM modes. This method places segmented conductors around the outside of the outermost dielectric layer. These segmented conductors interrupt the azimuthal surface currents which are needed to support the magnetic component of HEM modes. But for the TM modes which require longitudinal currents, these conductors are still capable of confining the wave and thus have no influence on the TM modes. Therefore, the HEM modes will not be confined within the segmented conductors. If we then surround the segmented conductors with a lossy material, the parasitic modes will be highly attenuated.

The matrix equation (4) is again used to solve for the HEM modes in the multilayer DLA waveguide. Some results for the parasitic modes for the same 4-layer DLA structure example are shown in Table 2. The r and r/Q of the parasitic mode is calculated for a particle that

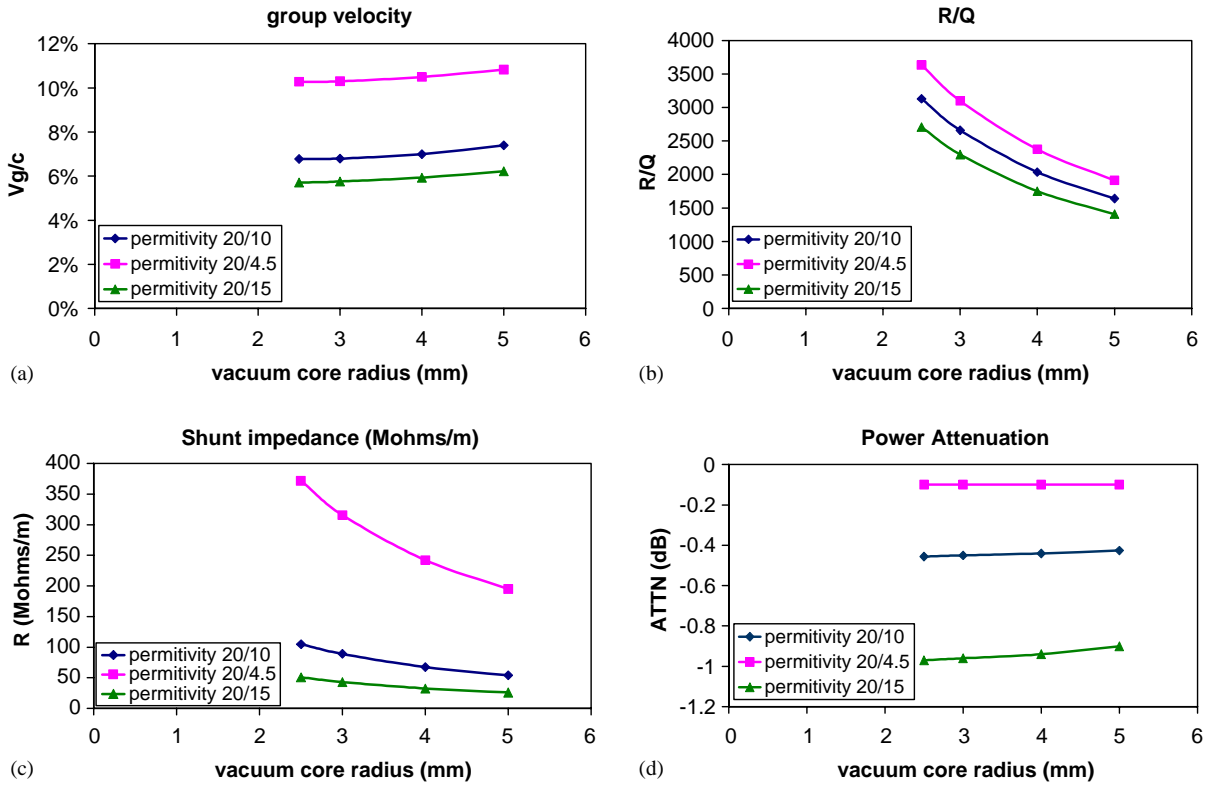


Fig. 5. Effect of both vacuum core size and dielectric permittivity ratio on four major accelerating parameters. Still, this model is based on 4-layer structure.

Table 2
Parasitic modes RF parameters comparison for multilayered and single layered DLA structures

	4-layer parasitic mode (HEM ₁₃)	Single-layer parasitic mode (HEM ₁₁)
Cut-off freq. (GHz)	11.886	9.2
Synchronized freq. (GHz)	12.28	9.87
Group velocity ($\times c$)	0.067	0.06
Q	33638	2623
r ($M\Omega/m/mm$)	2	0.1
r/Q ($\Omega/m/mm$)	60	40
Power attn (dB/m)	0.5	5.7

Geometric parameters for 4-layer DLA structure: radius of each layer is, in sequence, $b_0 = 3$ mm, $b_1 = 5.99$ mm, $b_2 = 8.3$ mm, $b_3 = 9.8$ mm, $b_4 = 12.1$ mm; single-layer DLA structure using TM₀₁ as accelerating mode: $b_0 = 3$ mm, $b_1 = 4.567$ mm. The r and r/Q of the parasitic mode is calculated for a particle that is 1 mm off-axis (given in units of MV/m/mm).

is 1 mm off-axis (given in units of MV/m/mm). Note that we use a complex permeability for outside lossy material layer in the parasitic mode

damping case. We use the numerical solver to find the complex propagation constants of each mode directly.

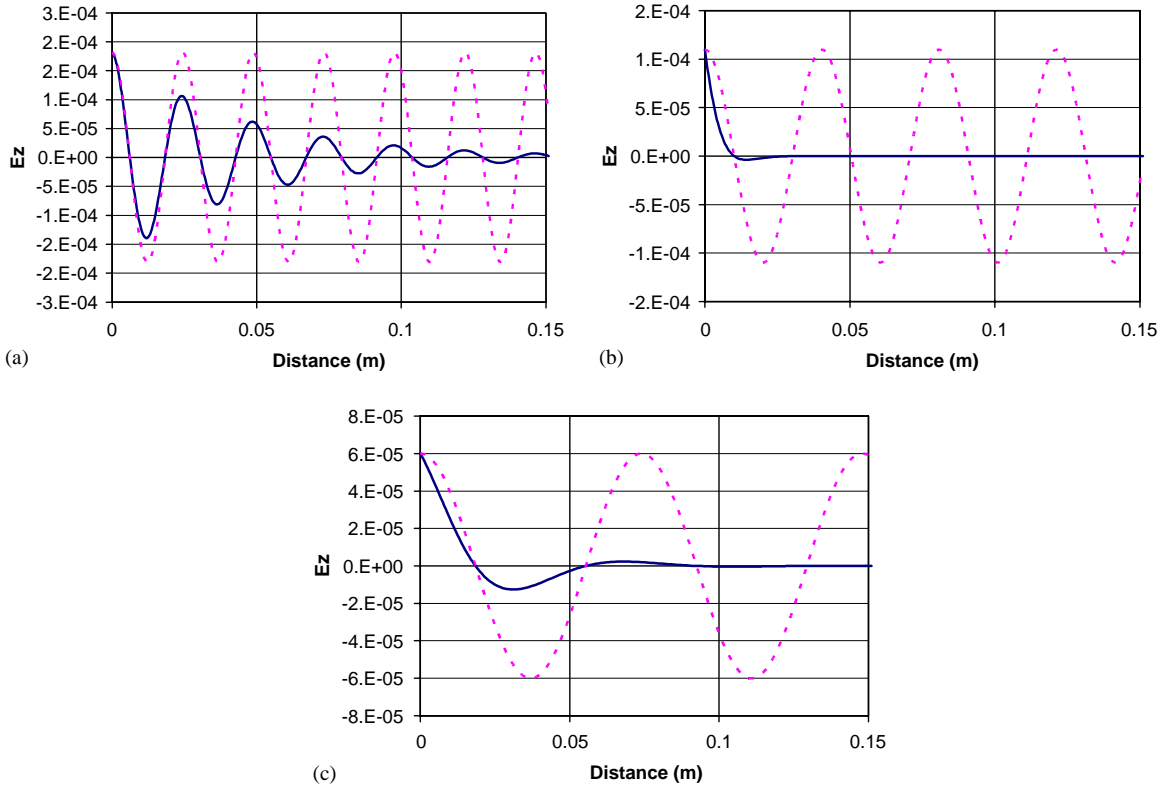


Fig. 6. Parasitic modes damping by thin ferrite foil. Dashed lines represent longitudinal electric field without damping and solid lines are those after damping.

Solving the complex transcendental equations for the multilayer structure is not an easy job. Fortunately, a similar damping scheme was undertaken by Chou and Lee [20] that demonstrates that, even without a segmented conductor, a thin ferrite film can suppress the HEM modes. In this case, since the lossy foil is very thin, we can apply perturbation theory and achieve acceptable accuracy. The complex propagation constant perturbation for a ferrite-loaded-waveguide problem can be expressed as [21]

$$\gamma + \gamma_0^* = \frac{j\omega \int_{\Delta S} (\Delta\epsilon \vec{E} \cdot \vec{E}_0^* + \Delta\mu \vec{H} \cdot \vec{H}_0^*) dS}{\int_S \vec{\alpha}_Z \cdot (\vec{E} \times \vec{H}_0^* + \vec{E}_0^* \times \vec{H}) dS} \quad (11)$$

where the complex propagation constant is $\gamma = \alpha + j\beta$, in which α represents attenuation constant and β propagation constant. Subscript 0 means the

unperturbed electromagnetic fields. If the filling factor (percentage of filling material in whole volume) is very small, less than 3 percent, we can obtain very accurate results.

Some results are shown in Fig. 6. The ferrite foil used to suppress the HEM modes is 0.2 mm thick, with a complex permeability of $\mu = 2 - j1.5$. The same geometry and electron beam source (1 mm off-axis particles) are used for the curves shown in Fig. 6; the dashed lines are for original waves and the solid lines are for the damped ones.

5. Conclusions

Using the concept of the bragg fiber, we proposed a multilayered dielectric-loaded accelerating (DLA) structure to reduce the attenuation of the accelerating mode compared to the single-layer

DLA structure. A recursive transfer matrix is applied in the mode analysis of this multilayered DLA structure. In a numerical example, we showed that the TM_{03} mode in the 4-layer DLA structure is the best operating acceleration mode due to its high shunt impedance and low field attenuation. Unlike the TM_{03} mode in single layer DLA structure, this TM_{03} mode in 4-layer DLA structure not only lowered the attenuation but also increased the shunt impedance which shows it has excellent potential use as an accelerator. The parasitic modes, which are generated by off-axis particles, can be easily damped. Further studies, such as effective high order mode coupling, and method of fabrication, are needed before this device could be implemented as a practical DLA structure.

References

- [1] P. Zou, W. Gai, R. Konecny, X. Sun, *Rev. Sci. Instrum.* 71 (2000) 2301.
- [2] W. Gai, P. Schoessow, B. Cole, R. Konecny, J. Norem, J. Rosenzweig, J. Simpson, *Phys. Rev. Lett.* 61 (1988) 2756.
- [3] J.G. Power, W. Gai, S.H. Gold, A.K. Kinkead, R. Konecny, C. Jing, W. Liu, Z. Yusof, *Phys. Rev. Lett.* 92 (2004) 164801.
- [4] Pochi Yeh, A. Yariv, *J. Opt. Soc. Am.* 68 (1978) 1196.
- [5] M. Ibanescu, S.G. Johnson, M. Soljacic, J.D. Joannopoulos, Y. Fink, O. Weisberg, T.D. Engeness, S.A. Jacobs, M. Skorobogatiy, *Phys. Rev. E* 67 (2003) 046608.
- [6] J.A. Harrington, *Fiber Integrated Opt.* 19 (2000) 211.
- [7] S.G. Johnson, M. Ibanescu, M. Skorobogatiy, O. Weisberg, T.D. Engeness, M. Soljacic, S.A. Jacobs, J.D. Joannopoulos, Y. Fink, *Opt. Express* 9 (2001) 749.
- [8] Yong Xu, R.K. Lee, A. Yariv, *Opt. Lett.* 25 (2000) 1756.
- [9] Yong Xu, G.X. Ouyang, R.K. Lee, A. Yariv, *J. Lightwave Tech.* 20 (2002) 428.
- [10] Mitsunobu Miyagi, Akihito Hongo, Shojiro Kawakami, *IEEE J. Quantum Electron.* QE-19 (1983) 136.
- [11] Mitsunobu Miyagi, Shojiro Kawakami, *J. Lightwave Tech.* 2 (1984) 116.
- [12] L. Schachter, R.L. Byer, R.H. Siemann, *Phys. Rev. E* 68 (2003) 036502.
- [13] A. Mizrahi, L. Schachter, R.L. Byer, R.H. Siemann, in: *Proceedings of the 2003 Particle Accelerator Conference* Portland, OR, Joe Chew, P. Lucas, S. Webber (Eds.), p. 728–730.
- [14] Private communications with Jay Hirshfield.
- [15] Refer to Ref. [4], and notice the term of $1/x$ in Eq. (37) of Ref. [4] should be $k_2/k_1^2\rho$.
- [16] Wei Gai, Ching-Hung Ho, *J. Appl. Phys.* 70 (1991) 3955.
- [17] T. Wangler, *RF Linear Accelerators*, Wiley, New York, 1998.
- [18] H.H. Braun, et al. CERN-CLIC-Note 364, 1998, unpublished.
- [19] L. Xiao, W. Gai, X. Sun, *Phys. Rev. E* 65 (2002) 016505.
- [20] Ri-Chee Chou, Shung-Wu Lee, *IEEE Tran. MTT* 36 (1988) 1167.
- [21] B. Lax, K.J. Button, *Microwave Ferrites and Ferrimagnetics* McGraw-Hill, New York, 1962 (Chapter 8).